ChemPubSoc Europe

DOI: 10.1002/open.201900167

Open Access ChemistryOPEN Full Papers

Solution-Based Determination of Dissociation Constants for the Binding of Aβ42 to Antibodies

Tao Zhang,[a, b] Luitgard Nagel-Steger,*[a, b] and Dieter Willbold[a, b]

Amyloid β-peptides (Aβ) play a major role in the pathogenesis of Alzheimer's disease. Therefore, numerous monoclonal antibodies against Aβ have been developed for basic and clinical research. The present study applied fluorescence based analytical ultracentrifugation and microscale thermophoresis to characterize the interaction between Aβ42 monomers and three popular, commercially available antibodies, namely 6E10, 4G8 and 12F4. Both methods allowed us to analyze the interactions at low nanomolar concentrations of analytes close to their dissociation constants (K_D) as required for the study of high affinity interactions. Furthermore, the low concentrations minimized the unwanted self-aggregation of Aβ. Our study demonstrates that all three antibodies bind to Aβ42 monomers with comparable affinities in the low nanomolar range. K_D values for Aβ42 binding to 6E10 and 4G8 are in good agreement with formerly reported values from SPR studies, while the K_D for 12F4 binding to Aβ42 monomer is reported for the first time.

1. Introduction

The aggregation of amyloid β-peptides (Aβ) into toxic oligomeric assemblies and fibrillar structures has been suggested to play an important role in the pathogenesis of Alzheimer's disease (AD).[1] Aβ is the proteolytic product of the amyloid precursor protein. It is the main component of amyloid deposits in brains of Alzheimer's patients.[2] A multitude of strategies has been developed to characterize and counteract Aβ pathologies in vivo, in an attempt to achieve early diagnosis and intervention of AD. Antibodies directed against Aβ are important tools for the characterization of Aβ species and have been proposed for the treatment of Aβ related pathologies. For example, monoclonal anti-Aβ antibodies are widely applied in enzyme-linked immunosorbent assay (ELISA), western blot or immunohistochemistry to determine Aβ proteins in cerebrospinal fluid, blood or tissue samples.[3] Several antibodies have been and are being tested in different stages of clinical trials to evaluate their efficacies on the cognitive performance of AD patients.[4] These antibodies recognize different epitopes of Aβ and some of them are claimed to be able to discriminate between different aggregation states of Aβ. For instance, Bapineuzumab targets the N-terminus (aa1-5) of Aβ and recognizes almost all kinds of Aβ species, including monomers, oligomers and fibrillar structures.[5] Solanezumab binds specifically to the central region of Aβ (aa16-23) responsible for the self-aggregation process and recognizes soluble Aβ species but not Aβ fibrils or amyloid plaques.[6] In addition to these antibodies for disease intervention, a number of anti-Aβ antibodies are broadly used as tools for basic research purposes. Considering the extensive and promising use of anti-Aβ antibodies in the field of AD research, it is necessary to quantitatively characterize the properties of antibodies recognizing different epitopes under near-physiological conditions to facilitate the application of these agents.

In vitro characterization of the interaction between Aβ and anti-Aβ antibodies is usually carried out using ELISA, surface plasmon resonance (SPR) or isothermal titration calorimetry (ITC), through which the binding affinities, kinetics or thermodynamics can be obtained.[3,7] X-ray crystallography has also been utilized to determine the high resolution structure of Aβ in complex with antibodies, albeit most studies chose Aβ fragments (N-terminus or the mid-region) or used Fab fragments for crystallization.[8] Since Aβ is highly flexible and prone to form aggregates already at low micromolar concentrations in aqueous solution, it is rather complicated to quantify the binding between antibodies and specific Aβ species, particularly the monomer, as a variety of Aβ species with different sizes and conformations may be present in solution. The impact of Aβ aggregation on the characterization might get pronounced in experiments requiring micromolar concentration of Aβ, such as ITC, putting aside the fact that for a reliable determination of binding constant the titrated concentrations should cover also the range of K_D. In SPR or ELISA measurements one of the analytes has to be immobilized on the surface of a sensor chip or a plate. In the case of surface immobilized Aβ species, one might encounter surface induced conformational changes, crowding effects or changes in the epitope accessibility.[9] In the complementary set-up, where the antibody is immobilized, the self-aggregation of Aβ at high concentrations is still inevitable.

[a] T. Zhang, Dr. L. Nagel-Steger, Prof. Dr. D. Willbold
Institute of Complex Systems, Structural Biochemistry (ICS-6)
Forschungszentrum Jülich
52425, Jülich, Germany
E-mail: l.nagel-steger@fz-juelich.de
[b] T. Zhang, Dr. L. Nagel-Steger, Prof. Dr. D. Willbold
Institut für Physikalische Biologie
Heinrich-Heine-Universität Düsseldorf
40225, Düsseldorf, Germany

Supporting information for this article is available on the WWW under https://doi.org/10.1002/open.201900167

Besides, the mass transport limitation in SPR might also need to be critically considered when dealing with high-affinity bindings.[10] One strategy to overcome these difficulties is to use fluorescently labeled molecules with solution based techniques so as to reduce the concentration of Aβ and antibodies to low nanomolar levels, so that the self-aggregation of Aβ will be significantly suppressed. Besides, it is also beneficial to the reliable determination of dissociation constants in the low nanomolar range. This could be helpful for the characterization of the interaction between Aβ monomers and anti-Aβ antibodies.

Analytical ultracentrifugation (AUC) is a solution based absolute method which has been widely used in characterizing macromolecules and protein-protein interactions. The development of the fluorescence based detection system permits the measurement of protein samples at picomolar to low nanomolar concentrations.[11] This high sensitivity in combination with a large dynamic range enables the study of high affinity interactions as found for antibody-antigen binding.[12] In contrast to AUC, microscale thermophoresis (MST) is a recently developed method based on the migration of macromolecules in response to thermal gradients.[13] This approach exploits the deviating thermophoretic behavior of a labeled molecule in the presence of different concentrations of its binding partner. By combining these two fluorescence based assays, we studied the interaction between fluorescein labeled Aβ42 (FITC-Aβ42) and three mAbs directed against Aβ (6E10, 4G8 and 12F4) to determine the antigen-antibody complex formation and binding affinities. Their epitopes of Aβ42 cover the N-terminus for 6E10, the C-terminus for 12F4, as well as the central hydrophobic core region for 4G8.

2. Results and Discussion

2.1. Complex Formation Between Aβ42 Monomers and Antibodies

We have initially characterized the size distributions of Aβ42 and the individual antibody using the sedimentation velocity measurement with different detection systems. Aβ42 monomer is an intrinsically disordered protein in aqueous solution. The $s_{20,w}$ of fluorescein isothiocyanate-β-Alanine labeled Aβ42 (FITC-Aβ42) as measured by the fluorescence detection system is 0.81 ± 0.02 S and the weight-average frictional ratio is 1.44 ± 0.1, suggesting a relatively elongated conformation.[14] It is also clear from the distribution that 40 nM FITC-Aβ42 did not form aggregates during the centrifugation process. The antibody 6E10 showed an $s_{20,w}$ of 7.2 S, additionally a small fraction, ~5% of an antibody dimer with $s_{20,w}$ of 11.7 S was detected by the absorbance based AUC measurement (Figure S1). The oligomerization of antibodies is a well-known general property, which for example plays a critical role in determining the shelf life of commercially manufactured antibodies.[15] The weight-average frictional ratio of 6E10 was 1.24, pointing to a globular shape of the antibody in solution.

In the presence of antibodies, FITC-Aβ42 formed complexes with the binding partner in a concentration dependent manner, as shown in Figure 1. The amount of unbound FITC-Aβ42 (found at ~0.8 S) decreased with increasing amounts of added antibody, while the antigen-antibody complex at ~7 S (Table 1) accumulated gradually with the titration of antibodies to the FITC-Aβ42 solution. In addition, we also observed a minor population of species with larger *s*-values in almost all antibody-containing samples. We speculate that these species most likely contain complexes formed by FITC-Aβ42 and antibody dimers. The complex of FITC-Aβ42 and dimeric antibody should sediment with about 11 S, very close to the *s*-value of an antibody dimer alone. Regarding the main complex at ~7 S, it is evident that there is only one antibody molecule bound to

Table 1. Weight-average $s_{20,w}$ of the major complex formed by antibodies and FITC-Aβ42.[a]

	6E10	4G8	12F4
Weight-average $s_{20,w}$ (S)	6.8 ± 0.4	6.8 ± 0.4	6.9 ± 0.3

[a] Values were determined by peak integration of the *c*(*s*) distribution from 4 to 10 S using GUSSI (version 1.2.1) and were expressed as mean ± S.D.

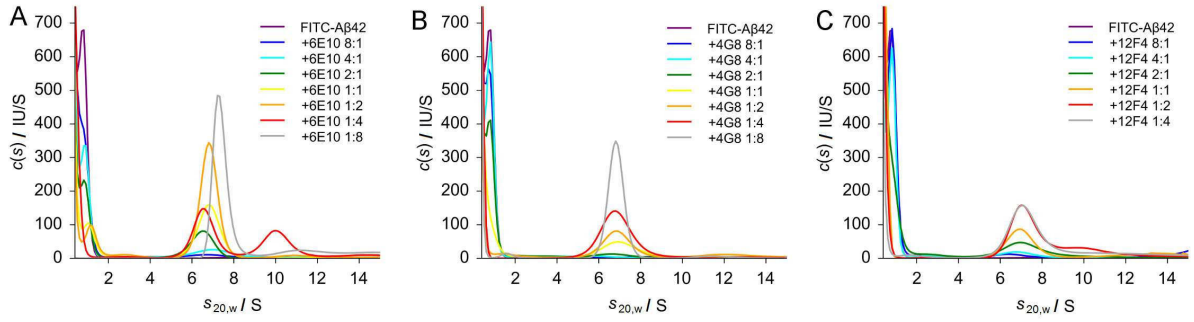

Figure 1. Sedimentation velocity analysis of FITC-Aβ42 in the presence of varying concentrations of three anti-Aβ antibodies. FITC-Aβ42 at 40 nM was titrated with 6E10 (A), 4G8 (B) and 12F4 (C) in 20 mM sodium phosphate, 50 mM NaCl (pH 7.4), 0.005% (v/v) Tween-20. All samples were centrifuged at 50,000 rpm (201,600 *g*) and 20 °C for 15 h. The sedimentation coefficient distribution was obtained using the continuous distribution *c*(*s*) Lamm equation model. The standardized $s_{20,w}$ for 20 °C and water as a solvent is reported.

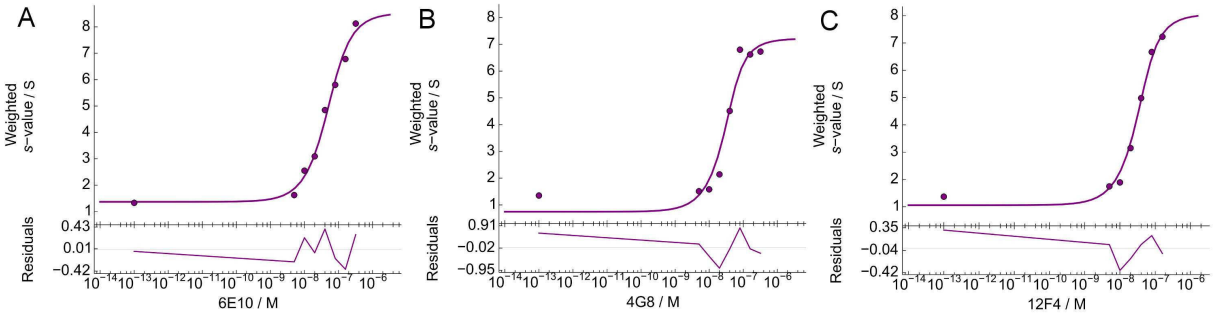

Figure 2. Binding isotherms of signal-weight average sedimentation coefficient (s_w) as a function of the logarithm of the loading concentration for 6E10 (A), 4G8 (B) and 12F4 (C). The isotherms were generated by integrating the distribution from 0.5 to 14 S according to the *c*(*s*) analysis and were fitted using the 'A + B⟷AB Hetero-Association' model implemented in Sedphat (version 10.58f) to determine the dissociation constants. For data evaluation, a concentration of 1×10^{-13} M of the antibody was assigned to samples of FITC-Aβ42 alone.

FITC-Aβ42, however, we cannot distinguish between antibodies that have one and two Aβ42 molecules bound, as the increase in the added molecule mass (4 kDa) to the mAb (150 kDa) cannot be resolved in the *s*-value regime. During the analysis we also noticed that the weight-average frictional ratio (f/f_0) of Aβ42-antibody mixtures decreased from about 1.5 for FITC-Aβ42 alone to about 1.2 in FITC-Aβ42 saturated with antibodies, which also hints the complexation between Aβ42 monomers and antibodies.

2.2. Determining the Dissociation Constants between Aβ42 Monomers and Antibodies Based on the Size Distributions

Next, we sought to determine the K_D values for each antibody based on the results from *c*(*s*) analyses. Note that the fluorescence signals of all samples in AUC measurements were constant over the measurement and were rather similar to each other, suggesting the absence of quenching or losing materials in the experiment. The complex formation between FITC-Aβ42 and antibody will lead to a gradual increase in the weight average *s*-value of the sample. Based on the mass action law, the signal-weight average sedimentation coefficient (s_w) isotherm can be built in order to determine the binding affinity.[11b] As can be seen from the fitting of the isotherms (Figure 2 and Table 2), all three antibodies form complexes with FITC-Aβ42 monomers with nanomolar affinities. The K_D determined for 6E10 and FITC-Aβ42 was 30.1 [13.2, 63.3] nM; the K_D values for 4G8 and 12F4 were 11.3 [1.0, 45.5] nM and 14.6 [4.7, 37.1] nM, respectively. In brackets the values obtained under 68.3% confidence interval are given.

2.3. Quantifying the Dissociation Constants Using Microscale Thermophoresis Analysis

To further investigate the interaction between FITC-Aβ42 and the antibodies, we carried out MST measurements using the same concentrations of FITC-Aβ42 and solvent conditions as used for AUC experiments. The thermophoretic behavior of a given target molecule can be influenced by changes in its size, charge and solvation upon binding to another molecule.[16] The fluorophore fluorescein alone did not interact with the antibody, as demonstrated by the control experiment (Figure S2), therefore any change in the thermophoresis could be attributed to the binding between Aβ42 monomers and the antibodies. The binding plots were analyzed via the simple 1:1 binding model despite the bivalent nature of the antibodies for two reasons. Firstly, using more complex models, for example the Hill model, could not improve the quality of the fit. Secondly, the titration of 40 nM Ab42 with the indicated concentrations of mAb will saturate only a single binding site. As shown in Figure 3 and Table 2, samples incubated with different antibodies exhibited different thermophoretic effects in MST measurements, although they are similar in size. The binding curve of FITC-Aβ42 and 6E10 revealed a K_D of 10.3 ± 4.6 nM. The descending trend of the normalized fluorescence (F_{norm}) in the presence of 6E10 suggested that bound FITC-Aβ42 molecules moved out of the heated zone faster than free molecules, indicating an increase in the thermophoretic mobility of FITC-Aβ42-6E10 complexes.[16] The K_D for FITC-Aβ42 and 4G8 was determined to be 12.8 ± 4.6 nM. Interestingly, the binding plot of FITC-Aβ42 and 4G8 displayed a pattern opposite to that of FITC-Aβ42 and 6E10, meaning that complexes had lower thermophoretic mobility than free FITC-Aβ42 molecules.[16] 12F4 bound to FITC-Aβ42 with a K_D of 9.5 ± 5 nM. The binding of 12F4 to FITC-Aβ42 also led to a decrease in the thermophoretic mobility, but to a lesser degree than that induced by 4G8. The

Table 2. A comparison of dissociation constants of the interaction between Aβ monomer and three monoclonal antibodies.

K_D (nM)	6E10	4G8	12F4
AUC[a]	30.1 [13.2, 63.3]	11.3 [1.0, 45.5]	14.6 [4.7, 37.1]
MST[b]	10.3 ± 4.6	12.8 ± 4.6	9.5 ± 5
SPR[c]	22.3	30.1	n/a

[a] Obtained based on fitting the isotherms of signal-weight average sedimentation coefficient (s_w) using the 'A + B⟷AB Hetero-Association' model and 68.3% confidence interval in Sedphat (version 10.58f). [b] Obtained according to the 1:1 binding model. [c] Obtained from SPR measurements in which Aβ40 monomers were injected over immobilized antibodies on the sensor chip and the 1:1 Langmuir binding model was used for data evaluation.[3]

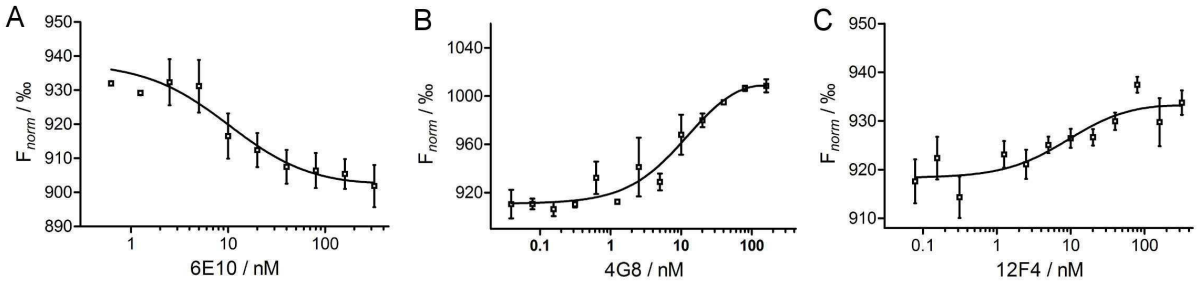

Figure 3. Microscale thermophoresis analysis of the interaction between FITC-Aβ42 and different antibodies. FITC-Aβ42 at 40 nM was titrated with different concentrations of antibodies in 20 mM sodium phosphate, 50 mM NaCl (pH 7.4), 0.005% (v/v) Tween-20 at ~23 °C. Binding plots of FITC-Aβ42 to 6E10 (A), 4G8 (B) and 12F4 (C) were fitted using the 1:1 binding model. Measurements were performed in triplicate.

reason for the deviation in the thermophoretic behavior of three Aβ42-antibody complexes is not clear yet. The antibodies used in the study recognize different epitopes of Aβ42 monomer. One possibility is that different degrees of post-translational modifications of the antibodies like glycosylation influence their thermophoretic behavior. According to literature 4G8 carries sialic acids on its surface, while 6E10 does not.[17] Additionally, the binding of antibodies to different regions of Aβ42 might induce alterations in the hydration shell of the complex, subsequently leading to different thermophoresis effects.[18]

Since the concentration of fluorescently labeled molecule is usually very low in fluorescence based measurements, it might be necessary to block the unspecific surface adsorption of the target molecule to maintain the input concentration. Therefore additives such as carrier proteins or detergents have been suggested for AUC or MST to deal with this problem.[11b,18] However, carrier proteins that are commonly used in fluorescence based AUC are not considered in the present study to avoid potential interference of these proteins with the interaction between antibodies and Aβ.[19] Tween-20 (0.005%, v/v) was thus used as an alternative to overcome the surface adsorption of FITC-Aβ42 in both experiments. Comparing dissociation constants measured in the present study with reported values from literature (Table 2), we found that the determined dissociation constants for all tested antibodies are in general agreement with those from literature, regardless of the methodology. Additionally, the three antibodies have rather similar affinities toward Aβ42 monomers, irrespective of the recognized epitopes. In light of the bivalent nature of the IgG antibody, it has been suggested in previous SPR studies that a bivalent model might be necessary to properly fit the data, especially when Aβ is immobilized on sensor chips .[7b] Nevertheless, the 1:1 binding model appears to be sufficient to fit the SPR data reasonably well in the case of Aβ binding to immobilized antibodies.[3] This indicates that the antibody might bind to Aβ monomers exclusively either with a single site or with both sites.[7b] It should be mentioned that both AUC and MST report the information about the bound and unbound states of the labeled molecule. At a concentration lower than the critical aggregation concentration of about 90 nM,[20] Aβ is unlikely to form aggregates within the time scale of both experiments, which definitely helps to reduce the incidence of multiple binding between Aβ oligomers and antibodies. The size distribution of all antibody-containing FITC-Aβ42 samples also revealed that complexes with only one antibody molecule were the dominant species in solution. Therefore, the simple 1:1 binding model also provided reasonable fitting results with good residuals in our study.

3. Conclusions

The combination of fluorescent labeling and solution based methods allows us to investigate the interaction between the aggregation-prone Aβ42 monomer and its binding partners in the concentration range of their dissociation constants. We obtained reliable binding parameters which are in good agreement with SPR studies on Aβ and antibodies. Besides, the dissociation constant between 12F4 and Aβ42 monomer was reported for the first time based on our measurements. The determined values may offer additional information for the application of these antibodies. AUC and MST are also capable of analyzing challenging samples such as tissue lysates, blood serum or other biological liquids,[21] which envisions the possible translation of the approach to physiological samples. However, solution based methods also have some limitations. For example, the fluorophore tag might have an impact on the interaction process by modifying the epitope or interacting directly with the binding partner. However, neither of the possibilities was evident in this study. Nevertheless, the rapid aggregation of Aβ oligomers in solution still renders it challenging to characterize the interaction between oligomeric species and antibodies via these solution based methods. Taken together, we demonstrate that AUC and MST can be useful and rigorous complements to surface based techniques for studying the interaction between Aβ species and various ligands.

Experimental Section

Chemicals

Fluorescein isothiocyanate-β-Alanine labeled Aβ42 (FITC-Aβ42) was purchased from Bachem (Catalog Number M-2585.1000, Weil am Rhein, Germany). The labeling was prepared by conjugating the fluorophore FITC to the amine group of the additional β-Alanine residue at the N-terminus of Aβ42. The purity of the FITC-Aβ42 product was 88.8%, according to the HPLC determination of the manufacturer. The molecular mass of the labeled molecule is 4974.4 Da, as determined by electrospray ionization mass spectrometry (ESI-MS). The HPLC and MS results (Figures S3 and S4) provided by the manufacturer can be found in the supporting information. Purified antibodies 6E10, 4G8 and 12F4 were obtained from BioLegend (San Diego, CA, USA). All antibodies are mouse derived monoclonal antibodies and are reactive to human Aβ proteins with different epitopes (Table S1). 1, 1, 1, 3, 3, 3-hexafluoro-2-propanol (HFIP) other chemicals are commercially available from Sigma-Aldrich (Munich, Germany). Aβ42 products (1 mg) were incubated in HFIP overnight at room temperature and were divided into small aliquots. HFIP was then removed and Aβ42 proteins were stored at −80 °C before use. All samples were prepared in 20 mM sodium phosphate, 50 mM NaCl at pH 7.4, with the addition of 0.005% (v/v) Tween-20.

Sedimentation Velocity Analytical Ultracentrifugation Analysis

Sedimentation velocity (SV) analysis of the fluorescent samples was performed using a Beckman Optima XL–A centrifuge (Beckman-Coulter, Brea, CA, USA) equipped with an 8-hole rotor and a fluorescence detection system (Aviv, Lakewood, NJ, USA). FITC-Aβ42 stock was mixed with antibody stock solutions to prepare samples with 40 nM FITC-Aβ42 and different concentrations of the antibody in 20 mM sodium phosphate, 50 mM NaCl (pH 7.4), 0.005% (v/v) Tween-20. Samples were then loaded into 3-mm double-sector titanium cells, with 100 µl per sample. Afterwards, all samples were thermally equilibrated to 20 °C in the centrifuge before the experiment. The centrifugation was carried out at 50,000 rpm (201,600 *g*) and 20 °C for 15 h. The detection system uses an excitation wavelength at 488 nm and an emission cut-off filter at 505 nm for data acquisition. The sedimentation profiles were analyzed using the software package Sedfit (version 15.01b) and the continuous distribution *c(s)* Lamm equation model to obtain the sedimentation coefficient (*s*-value) distribution.[22] Buffer density and viscosity (Table S2) were calculated using Sednterp (version 20130813BETA). The partial specific volume ($\bar{\nu}$) of FITC-Aβ42 was determined according to Sednterp and Durchschlag et al.[23] For mixtures of Aβ42 and antibodies, a partial specific volume ($\bar{\nu}$) of 0.73 cm^3/g was used for the calculation of *s*-value. The final graphs of the sedimentation coefficient distribution were created by GUSSI (version 1.2.1),[24] with all *s*-values standardized to $s_{20,w}$ (*s*-value at 20 °C and water as a solvent). The isotherm of weight average $s_{20,w}$ as a function of the loading concentration (s_w) for each antibody was created by integrating the distribution from 0.5 to 14 S in GUSSI.[11b] The isotherms were further analyzed in Sedphat (version 10.58f) using the 'A + B⟷AB Hetero-Association' model with a confidence interval of 68.3% to determine the K_D values.[25] The fitted binding plots were displayed via GUSSI.[24]

The size distribution of the antibody alone was also evaluated via analytical ultracentrifugation with an absorbance detection system. In brief, the 6E10 antibody was prepared in 20 mM sodium phosphate, 50 mM NaCl (pH 7.4) to obtain a concentration of 1.2 µM. Antibody samples at 380 µl were then loaded into a 12-mm double-sector aluminum cell. After thermal equilibration samples were centrifuged at 40,000 rpm (129,024 *g*), 20 °C. The sedimentation was monitored using a detection wavelength at 230 nm and a step size of 20 µm. The density and viscosity of the buffer were calculated according to Sednterp (version 20130813BETA). The partial specific volume of the antibody was assumed to be 0.73 cm^3/g. The size distribution was determined using the continuous distribution *c(s)* Lamm equation model implemented in Sedfit (version 15.01b).[22]

Microscale Thermophoresis

The binding between FITC-Aβ42 and antibodies was characterized using microscale thermophoresis to determine the dissociation constant (K_D). FITC-Aβ42 at 40 nM was titrated with different concentrations of antibody solutions in 20 mM sodium phosphate, 50 mM NaCl (pH 7.4), 0.005% (v/v) Tween-20. Samples were immediately transferred to standard capillaries (NanoTemper, Munich, Germany) and the thermophoresis was measured by a Monolith NT.115 system from the same manufacturer at room temperature (~23 °C). The excitation light of the LED was chosen according to the fluorophore of the labeled molecule. The LED power and the infrared (IR) laser power were set to 40% and 50%, respectively. The on- and off-phase of the IR laser was set to 30 s and 5 s, respectively. F_{norm} was plotted against the logarithm titrant concentrations to obtain the binding plots. The K_D value for each antibody was reported based on the fitting of a 1:1 binding model via OriginPro (version 9.0.0).

A control MST experiment was performed by titrating 40 nM fluorescein with the same concentration of 6E10 as has been used in experiments on FITC-Aβ42. The measurement was conducted under the same condition.

Acknowledgements

This work receives financial support from the Helmholtz Association through the Helmholtz-Portfolio Topic "Technology and Medicine" (D.W., L.N.-S.). T. Z. thanks the support from the China Scholarship Council (CSC) and the iGRAPseed graduate school of Heinrich-Heine-Universität Düsseldorf.

Conflict of Interest

The authors declare no conflict of interest.

Keywords: amyloid β-peptides · analytical ultracentrifugation · microscale thermophoresis · monoclonal antibodies · protein-protein interactions

[1] A. Serrano-Pozo, M. P. Frosch, E. Masliah, B. T. Hyman, *Cold Spring Harbor Perspect. Med.* **2011**, *1*, a006189.
[2] S. J. Lee, E. Nam, H. J. Lee, M. G. Savelieff, M. H. Lim, *Chem. Soc. Rev.* **2017**, *46*, 310–323.
[3] M. Ramakrishnan, K. K. Kandimalla, T. M. Wengenack, K. G. Howell, J. F. Poduslo, *Biochemistry* **2009**, *48*, 10405–10415.
[4] G. Gallardo, D. M. Holtzman, *Cold Spring Harbor Perspect. Med.* **2017**, *7*.
[5] S. Salloway, R. Sperling, N. C. Fox, K. Blennow, W. Klunk, M. Raskind, M. Sabbagh, L. S. Honig, A. P. Porsteinsson, S. Ferris, M. Reichert, N. Ketter, B. Nejadnik, V. Guenzler, M. Miloslavsky, D. Wang, Y. Lu, J. Lull, I. C.

Tudor, E. Liu, M. Grundman, E. Yuen, R. Black, H. R. Brashear, Bapineuzumab, I. Clinical Trial, *N. Engl. J. Med.* **2014**, *370*, 322–333.
[6] R. S. Doody, R. G. Thomas, M. Farlow, T. Iwatsubo, B. Vellas, S. Joffe, K. Kieburtz, R. Raman, X. Sun, P. S. Aisen, E. Siemers, H. Liu-Seifert, R. Mohs, C. Alzheimer's Disease Cooperative Study Steering, G. Solanezumab Study, *N. Engl. J. Med.* **2014**, *370*, 311–321.
[7] a) B. O'Nuallain, L. Acero, A. D. Williams, H. P. Koeppen, A. Weber, H. P. Schwarz, J. S. Wall, D. T. Weiss, A. Solomon, *Biochemistry* **2008**, *47*, 12254–12256; b) A. C. Crisostomo, L. Dang, J. L. Digambaranath, A. C. Klaver, D. A. Loeffler, J. J. Payne, L. M. Smith, A. L. Yokom, J. M. Finke, *Anal. Biochem.* **2015**, *481*, 43–54; c) M. Brockhaus, P. Ganz, W. Huber, B. Bohrmann, H. R. Loetscher, J. Seelig, *J. Phys. Chem. B.* **2007**, *111*, 1238–1243; d) J. W. Arndt, F. Qian, B. A. Smith, C. Quan, K. P. Kilambi, M. W. Bush, T. Walz, R. B. Pepinsky, T. Bussiere, S. Hamann, T. O. Cameron, P. H. Weinreb, *Sci. Rep.* **2018**, *8*, 6412.
[8] a) A. Teplyakov, G. Obmolova, G. L. Gilliland, *Alzheimer's Res. Ther.* **2017**, *9*, 66; b) G. A. Crespi, D. B. Ascher, M. W. Parker, L. A. Miles, *Acta Crystallogr. Sect. F* **2014**, *70*, 374–377; c) G. A. Crespi, S. J. Hermans, M. W. Parker, L. A. Miles, *Sci. Rep.* **2015**, *5*, 9649; d) L. A. Miles, G. A. Crespi, L. Doughty, M. W. Parker, *Sci. Rep.* **2013**, *3*, 1302; e) S. L. La Porte, S. S. Bollini, T. A. Lanz, Y. N. Abdiche, A. S. Rusnak, W. H. Ho, D. Kobayashi, O. Harrabi, D. Pappas, E. W. Mina, A. J. Milici, T. T. Kawabe, K. Bales, J. C. Lin, J. Pons, *J. Mol. Biol.* **2012**, *421*, 525–536.
[9] M. Jin, B. O'Nuallain, W. Hong, J. Boyd, V. N. Lagomarsino, T. T. O'Malley, W. Liu, C. R. Vanderburg, M. P. Frosch, T. Young-Pearse, D. J. Selkoe, D. M. Walsh, *Nat. Commun.* **2018**, *9*, 2676.
[10] P. Schuck, H. Zhao, *Methods Mol. Biol.* **2010**, *627*, 15–54.
[11] a) I. K. MacGregor, A. L. Anderson, T. M. Laue, *Biophys. Chem.* **2004**, *108*, 165–185; b) H. Zhao, M. L. Mayer, P. Schuck, *Anal. Chem.* **2014**, *86*, 3181–3187; c) E. Krayukhina, M. Noda, K. Ishii, T. Maruno, H. Wakabayashi, M. Tada, T. Suzuki, A. Ishii-Watabe, M. Kato, S. Uchiyama, *mAbs* **2017**, *9*, 664–679.
[12] R. R. Kroe, T. M. Laue, *Anal. Biochem.* **2009**, *390*, 1–13.
[13] M. Jerabek-Willemsen, C. J. Wienken, D. Braun, P. Baaske, S. Duhr, *Assay Drug Dev. Technol.* **2011**, *9*, 342–353.
[14] P. H. Brown, A. Balbo, P. Schuck, *Curr. Protoc. Immunol.* **2008**, *Chapter 18*, 18.15.11–18.15.39.
[15] T. Skamris, X. Tian, M. Thorolfsson, H. S. Karkov, H. B. Rasmussen, A. E. Langkilde, B. Vestergaard, *Pharm. Res.* **2016**, *33*, 716–728.
[16] S. Duhr, D. Braun, *Proc. Natl. Acad. Sci. USA* **2006**, *103*, 19678–19682.
[17] a) H. Kwon, A. C. Crisostomo, H. M. Smalls, J. M. Finke, *PLoS One* **2015**, *10*, e0120420; b) J. M. Finke, K. R. Ayres, R. P. Brisbin, H. A. Hill, E. E. Wing, W. A. Banks, *Biochim. Biophys. Acta Gen. Subj.* **2017**, *1861*, 2228–2239.
[18] S. A. Seidel, P. M. Dijkman, W. A. Lea, G. van den Bogaart, M. Jerabek-Willemsen, A. Lazic, J. S. Joseph, P. Srinivasan, P. Baaske, A. Simeonov, I. Katritch, F. A. Melo, J. E. Ladbury, G. Schreiber, A. Watts, D. Braun, S. Duhr, *Methods* **2013**, *59*, 301–315.
[19] a) A. A. Reyes Barcelo, F. J. Gonzalez-Velasquez, M. A. Moss, *J. Biol. Eng.* **2009**, *3*, 5; b) J. Luo, S. K. Warmlander, A. Graslund, J. P. Abrahams, *J. Biol. Chem.* **2014**, *289*, 27766–27775.
[20] M. Novo, S. Freire, W. Al-Soufi, *Sci. Rep.* **2018**, *8*, 1783.
[21] a) S. A. Kim, V. F. D'Acunto, B. Kokona, J. Hofmann, N. R. Cunningham, E. M. Bistline, F. J. Garcia, N. M. Akhtar, S. H. Hoffman, S. H. Doshi, K. M. Ulrich, N. M. Jones, N. M. Bonini, C. M. Roberts, C. D. Link, T. M. Laue, R. Fairman, *Biochemistry* **2017**, *56*, 4676–4688; b) C. J. Wienken, P. Baaske, U. Rothbauer, D. Braun, S. Duhr, *Nat. Commun.* **2010**, *1*, 100.
[22] J. Dam, C. A. Velikovsky, R. A. Mariuzza, C. Urbanke, P. Schuck, *Biophys. J.* **2005**, *89*, 619–634.
[23] H. Durchschlag, P. Zipper, *Prog. Colloid Polym. Sci.* **1994**, *94*, 20–39.
[24] C. A. Brautigam, *Methods Enzymol.* **2015**, *562*, 109–133.
[25] S. K. Chaturvedi, J. Ma, H. Zhao, P. Schuck, *Nat. Protoc.* **2017**, *12*, 1777–1791.

Manuscript received: May 10, 2019
Revised manuscript received: July 4, 2019